

# *International Review of Automatic Control (IREACO)*

Theory and Applications

## **Contents**

<b>DC Motor Control Using PID Controller Based on Improved Ant Colony Algorithm</b> <i>by H. E. A. Ibrahim, Ahmed A. Hakim Mahmoud</i>	1
<b>Literature Review on Microstepping Control for Permanent Magnet Stepper Motor</b> <i>by S. Vijaya, A. Senthil Kumar, R. Suganya</i>	7
<b>Real Time Implementation of Third Generation CRONE Control Strategy for DC Motor Speed Control System</b> <i>by N. N. Praboo, P. K. Bhaba</i>	15
<b>Recovery of HVDC System from DC Line Fault: a New Protection Method</b> <i>by M. Benasla, T. Allaoui, M. Brahmi</i>	23
<b>PID Controller Based Adaptive PSO</b> <i>by Adel Taieb, Abdelkader Chaari</i>	31
<b>Performance Evaluation of Self-Excited Induction Generators</b> <i>by M. Selmi, H. Rebaoulia</i>	38
<b>Modeling and Control of Mechatronic Systems Using Fuzzy Logic</b> <i>by Ján Čigánek, Filip Noge, Štefan Kozák</i>	45
<b>An ANN Control of Maximum Power Point Tracking for Grid Connected Wind Machines</b> <i>by S. Sundeep, G. Madbusudhana Rao, B. V. Sankar Ram</i>	52
<b>Evaluation of Space Vector Switching Patterns Based on Reference Functions and Switching Loss Factor in VSI Fed Induction Motor Drive</b> <i>by P. Senthilkumar, M. Balachandran, N. P. Subramaniam</i>	60
<b>Nonlinear Robust Sliding Mode Control of Flight Simulator (6-3) Gough-Stewart Type in Task Space</b> <i>by M. Litim, A. Omari</i>	67
<b>Predictive Trailing Triangle Modulation Peak Current Control in DC-DC Converters</b> <i>by Daniel Drăghici, Aurel Cireșan, Mircea Gurbină, Dan Lascu</i>	74
<b>Motion Planning and Control of Hyper Dynamic Robot Arm</b> <i>by S. Benmansour Aboura, A. Omari, K. Zemalache Meguenni</i>	82
<b>Identification of Lead-Acid Battery Parameters by Kalman Filter Using Various Battery Models</b> <i>by A. Boutte, A. Midoun</i>	90
<b>Robust Control of Twin Rotor MIMO System</b> <i>by S. Nekrouf, M. Bouhamida, Z. Bellabcen</i>	98
<b>Online Prediction Model Based on New Kernel Method</b> <i>by I. Elaissi, O. Taouali, H. Messaoud</i>	107
<b>Passivity-Based Analysis for Partially Variable Nonlinear PID Controller for Robot Manipulators</b> <i>by Sifuentes Mijares Juan, Meza Medina José Luis</i>	114



Praise Worthy Prize

# Nonlinear Robust Sliding Mode Control of Flight Simulator (6-3) Gough-Stewart Type in Task Space

M. Litim, A. Omari

**Abstract** – This paper presents a sliding mode control of a flight simulator Gough-Stewart type. The control is based on the inverse dynamic model of the robot in task space. Kinematic analysis is also discussed. High performance tracking control of a 6 DOF Stewart platform normally requires full knowledge of the system dynamics. In this paper, some important properties of the dynamics of the Stewart platform are considered to develop a sliding mode controller which can drive the upper platform angular and translation positions to the desired trajectories. Stability analysis based on Lyapunov theory is performed to ensure that the designed controller is stable. Numerical simulation is completed to show the effectiveness of the control system even in the case of large parameter variations. **Copyright © 2014 Praise Worthy Prize S.r.l. - All rights reserved.**

**Keywords:** Flight Simulator, Gough-Stewart Platform, Sliding Mode Control, Lyapunov Stability

## Nomenclature

$P = [xyz\alpha\beta\gamma]^T$	Operational vector
$\ddot{P} = [\ddot{x}\ddot{y}\ddot{z}\ddot{\alpha}\ddot{\beta}\ddot{\gamma}]^T$	Acceleration vector
$\Gamma = [\Gamma_1\Gamma_2\Gamma_3\Gamma_4\Gamma_5\Gamma_6]^T$	Input torque vector
$M(P)$	Inertia matrix expressed in Cartesian space
$C(P, \dot{P})$	Coriolis and centrifugal force/torque in Cartesian space
$J$	Jacobian matrix
$m$	Mass of upper plate
$G(P)$	Gravity acceleration
$S$	Sliding mode surfaces
$\lambda$	$6 \times 6$ diagonal positive definite matrix
$K \in R^{6 \times 1}$	Gain of sliding mode
$C(\cdot)$	$\cos(\cdot)$
$S(\cdot)$	$\sin(\cdot)$
$I(\cdot)$	Inertia of the platform

## I. Introduction

The Stewart platform Parallel link manipulators attract many researchers in the current decade, which have several advantages including high speed and precision and good capability of payload, therefore, they are applied to various fields. A Stewart platform is a parallel robot provides six-degree-of-freedom roll, pitch, yaw, surge, sway and heave.

Its practical usage is for disturbance isolation, precise machining and flight simulators. The Gough-Stewart platform manipulator is a mechanism has six variable-length electro-mechanical actuators connecting a top plate to a base plate with spherical joints [1], [2]. Angular and translation motion of the top plate with respect to the

base plate is produced by reducing or extending the actuator lengths.

The proper coordination of the actuators length enables the top plate to follow the desired trajectory with high accuracy. Thus the six inputs to the Stewart platform in term of torque are calculated by controller.

The outputs of the Stewart platform are the upper platform angular and translation positions.

In recent years, there have been some remarkable attempts to control the Gough-Stewart manipulator in the task space. The control strategies, based on the dynamic model of the Gough-Stewart platform, vary from a simple dynamic model regarding only the end effectors [3], [4], [5], or a simplified dynamic model with some considerations [6], to a complete dynamic model based on the Newton Euler or Lagrangian formalism, [7], [8], [9] and [10]. In [8] adaptive control law based on the full dynamics obtained with the Lagrangian formalism is applied. In [11] the dynamic model is obtained using the Newton-Euler approach. A robust adaptive controller for the Gough-Stewart is presented in [12].

Sliding mode control method exhibits the property of robustness which is able to withstand external disturbances and parameter uncertainties [13] [14]. so that it has been in use for control of various types of systems including linear and nonlinear systems, SISO and MIMO systems, discrete time models, large scale and infinite dimensional systems and stochastic systems [15]. Magnetic levitation in [16]. Robots manipulators presented in [17]. DC-DC converters in [18] [19]. Underwater vehicles [20] and photovoltaic solar in [21].

In this paper sliding mode controller for a nonlinear inverse dynamic model of platform in task space using the Lyapunov method is considered. The control is based on the inverse dynamic model in task space of Stewart platform (6-3) type using sliding mode control to drive

asymptotically the upper plate's angular and translation positions to the desired trajectories. The remainder of this paper is organized as follow. The kinematics and direct dynamics model of the Stewart platform are discussed in Section 2. In section 3 the sliding mode controller applied to the inverse dynamic model is developed. Section 4 shows the simulation results of a sliding mode controller (SMC).

Finally, section 5 concludes the results.

## II. Modeling of the Gough-Stewart Platform

### A. Kinematic and geometric modeling

For geometric modeling and kinematics of a Stewart platform type (6-3), the following conventions are used (Fig. 1).

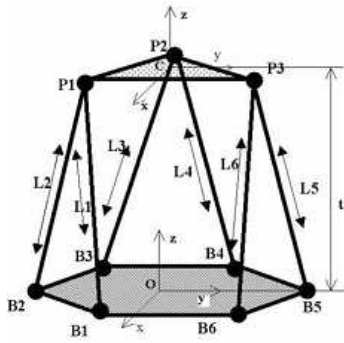


Fig. 1. Generalized (6-3) Stewart platform manipulator

The centers of the spherical and universal joints are designated by  $B_i$  ( $i = 1, 2 \dots 6$ ) and  $P_i$  ( $i = 1, 2 \dots 6$ ), respectively. The installation of the mobile platform is represented by six-operational variables: three variables ( $X, Y, Z$ ) for linear displacements along the three axes and three angles for orientation ( $\alpha, \beta, \gamma$ ).

The operational vector is then written:

$$P = [XYZ\alpha\beta\gamma]^T \quad (1)$$

Then the length of the leg is the amplitude of the vector  $B_iP_i$  is given by:

$$L_i = \|\overrightarrow{B_iP_i}\| = \|\overrightarrow{B_iO} + \overrightarrow{OC} + RCP_i^m\| \quad (2)$$

This is the inverse geometric formula that gives the length of each leg for a given desired position and orientation of the end effectors. The direct geometric model which give the position  $X, Y, Z$  and orientation angles  $\alpha, \beta, \gamma$  for a given measured value of  $L_i$ ,  $i = 1, 2 \dots 6$ . This model is nonlinear and is solved using numerical methods. The inverse kinematic model give the velocity of the active joint  $L_i$  for a given end effectors linear and angular velocity and is given as:

$$\dot{P} = J^{-1}\dot{L} \quad (3)$$

where  $J$  is a  $6 \times 6$  Jacobean matrix of the platform with respect to the base frame [7]:

$$\dot{L} = \begin{pmatrix} n_1^T (RCB_1^m \wedge n_1)^T \\ n_2^T (RCB_2^m \wedge n_2)^T \\ \vdots \\ n_6^T (RCB_6^m \wedge n_6)^T \end{pmatrix} \cdot \dot{P}$$

$\dot{P} = [\dot{X}\dot{Y}\dot{Z}\dot{\alpha}\dot{\beta}\dot{\gamma}]^T$ ,  $n_i$  is unit vector,  $R$  is rotation matrix.

### B. Dynamic modeling

The dynamic modeling of Stewart platform manipulator has been extensively studied by many researchers [7].

The methods used are Lagrange, Newton Euler and principle of virtual work [11]. Using Lagrange method, it can be written as:

$$\frac{d}{dt} \left( \frac{\partial K(P, \dot{P})}{\partial \dot{P}} \right) - \frac{\partial K(P, \dot{P})}{\partial P} + \frac{\partial Q}{\partial P} = \tau \quad (4)$$

Recently, the problem of control of robots has required a deeper analysis of the structure of this formulation. Thus, we will not directly use (4) but we use (5) which is derived from (4) [7].

The actuator torque  $\tau$  is given in task space [8] as:

$$M(P)\ddot{P} + C(P, \dot{P})\dot{P} + G(P) = J^T\Gamma \quad (5)$$

where  $M(P)$  is a  $6 \times 6$  inertia matrix, which is a symmetric and positive definite for all  $P \in R^6$ ;  $C(P, \dot{P})\dot{P}$  is the Coriolis/Centripetal vector;  $G(P)$  and  $\Gamma$  are  $6 \times 1$  vectors containing gravity torques and input torques, respectively. Some pertaining properties are given below.

*Property 1:*

$M(P)$  is bounded function if and  $P$  and  $\dot{P}$  are bounded.  
 $C(P, \dot{P})$  is a bounded function if, and  $P, \dot{P}, \ddot{P}$  are bounded.  
 $G(P)$  is bounded if  $P$  is bounded.

*Property 2:*

$M$  is a symmetric and positive definite matrix for all  $P \in R$  Moreover,  $\dot{M} - 2C$  is a skew-symmetric matrix, such that  $P^T(\dot{M} - 2C)P = 0 \quad \forall x \in R^n$

To obtain the kinetic and potential energies, the Stewart platform can be divided into two parts: the upper platform and six legs. In this study, it is assumed that the mass of each leg is too little than mass of upper platform then it can be neglected. For the upper platform the kinetic energy is the sum of the translation energy and the rotational energy of the body about the center of mass. We therefore obtain:

$$K(P, \dot{P}) = \frac{1}{2} m_{(mf)} (\dot{X}^2 + \dot{Y}^2 + \dot{Z}^2) + \frac{1}{2} \Omega_{(mf)}^T I_{(mf)} \Omega_{(mf)} \quad (6)$$

where  $m_{(mf)}$  is the mass of upper platform,  $I_{(mf)}$  is the tensor of inertia that is easy to write within a frame associated with the platform  $I_{(mf)} = \text{diag}\{I_x, I_y, I_z\}$  and  $\Omega_{(mf)}$  is the angular velocity of upper platform that it is defined within the TOP frame:

$$\Omega_{(mf)} = R_z(\gamma)^T R_x(\alpha)^T R_y(\beta)^T \Omega_{(ff)} \quad (7)$$

where  $\Omega_{(ff)}$  denotes the angular velocity of the moving platform with respect to the base frame.

$R_x(\alpha), R_y(\beta)$  and  $R_z(\gamma)$  represent the rotation matrices around x, y and z-axis.

Given the definition of the angles  $\alpha, \beta$  and  $\gamma$ , the angular velocity,  $\Omega_{(ff)}$  is:

$$\begin{aligned} \Omega_{(ff)} &= \dot{\alpha}R_y(\beta)X + \dot{\beta}Y + \dot{\gamma}R_x(\alpha)R_z(\gamma)Z = \\ &= \left( \begin{array}{c} \begin{bmatrix} \cos\beta & 0 & \sin\beta \\ 0 & 1 & 0 \\ -\sin\beta & 0 & \cos\beta \end{bmatrix} \begin{bmatrix} 1 & 0 & 0 \\ 0 & 0 & 0 \\ 0 & 0 & 0 \end{bmatrix} + \\ + \begin{bmatrix} 0 & 0 & 0 \\ 0 & 1 & 0 \\ 0 & 0 & 0 \end{bmatrix} + \begin{bmatrix} 1 & 0 & 0 \\ 0 & \cos\alpha & -\sin\alpha \\ 0 & \sin\alpha & \cos\alpha \end{bmatrix} \cdot \begin{bmatrix} \dot{\alpha} \\ \dot{\beta} \\ \dot{\gamma} \end{bmatrix} \\ \cdot \begin{bmatrix} \cos\gamma & -\sin\gamma & 0 \\ \sin\gamma & \cos\gamma & 0 \\ 0 & 0 & 1 \end{bmatrix} \begin{bmatrix} 0 & 0 & 0 \\ 0 & 0 & 0 \\ 0 & 0 & 1 \end{bmatrix} \end{array} \right) \begin{bmatrix} \dot{\alpha} \\ \dot{\beta} \\ \dot{\gamma} \end{bmatrix} = \\ &= \begin{bmatrix} \cos\beta & 0 & 0 \\ 0 & 1 & -\sin\alpha \\ -\sin\beta & 0 & \cos\alpha \end{bmatrix} \begin{bmatrix} \dot{\alpha} \\ \dot{\beta} \\ \dot{\gamma} \end{bmatrix} \quad (8) \end{aligned}$$

In the moving platform coordinate system, the angular velocity of the moving platform given in Eq. (7) is calculated as:

$$\begin{aligned} \Omega_{(mf)} &= \\ &= \begin{bmatrix} c\gamma & cas\gamma & -cac\gamma s\beta - cas\alpha s\gamma + cac\beta s\alpha s\gamma \\ -s\gamma & cac\gamma & -cac\gamma s\alpha + cas\beta s\gamma + cac\beta s\alpha c\gamma \\ 0 & -s\alpha & s^2\alpha + c^2\alpha c\beta \end{bmatrix} \begin{bmatrix} \dot{\alpha} \\ \dot{\beta} \\ \dot{\gamma} \end{bmatrix} \end{aligned}$$

where  $s(\cdot) = \sin(\cdot)$  and  $c(\cdot) = \cos(\cdot)$ . As a result, the total kinetic energy of the moving platform in a compact form is given by:

$$\begin{aligned} K &= K_{(trans)} + K_{(rot)} = \frac{1}{2} m_{mf} (\dot{X}^2 + \dot{Y}^2 + \dot{Z}^2) + \\ &+ \frac{1}{2} \Omega_{(mf)}^T I_{(mf)} \Omega_{(mf)} \end{aligned}$$

The potential energy of the Stewart platform is easy to express as:

$$Q = mgZ = \begin{bmatrix} 0 \\ 0 \\ mg \\ 0 \\ 0 \\ 0 \end{bmatrix}^T \begin{bmatrix} X \\ Y \\ Z \\ \alpha \\ \beta \\ \gamma \end{bmatrix} = [0 \ 0 \ mg \ 0 \ 0 \ 0]P \quad (9)$$

The inertial matrix  $M$  can be written as:

$$M = \begin{bmatrix} m & 0 & 0 & 0 & 0 & 0 \\ 0 & m & 0 & 0 & 0 & 0 \\ 0 & 0 & m & 0 & 0 & 0 \\ 0 & 0 & 0 & M_{44} & M_{45} & M_{46} \\ 0 & 0 & 0 & M_{54} & M_{55} & M_{56} \\ 0 & 0 & 0 & M_{64} & M_{65} & M_{66} \end{bmatrix}$$

$$M_{44} = I_x C_\beta^2 C_\gamma^2 + I_x C_\beta^2 S_\gamma^2 + I_y S_\beta^2$$

$$M_{45} = M_{54} = (I_x - I_y) C_\beta C_\gamma S_\gamma$$

$$M_{46} = M_{64} = I_z S_\beta$$

$$M_{55} = I_x S_\gamma^2 + I_y C_\gamma^2$$

$$M_{66} = I_z$$

The Coriolis-Centrifugal matrix can be written as:

$$C = \begin{bmatrix} 0 & 0 & 0 & 0 \\ 0 & 0 & 0 & 0 \\ 0 & 0 & 0 & 0 \\ 0 & 0 & 0 & -K_1 \dot{\beta} - K_2 \dot{\gamma} \\ 0 & 0 & 0 & K_1 \dot{\alpha} + K_4 \dot{\gamma} \\ 0 & 0 & 0 & K_2 \dot{\alpha} - K_4 \dot{\beta} \\ 0 & 0 & 0 & 0 \\ 0 & 0 & 0 & 0 \\ 0 & 0 & 0 & 0 \\ -K_1 \dot{\alpha} - K_3 \dot{\beta} + K_4 \dot{\gamma} & -K_2 \dot{\alpha} + K_4 \dot{\beta} \\ K_5 \dot{\gamma} & K_4 \dot{\alpha} + K_5 \dot{\beta} \\ -K_4 \dot{\alpha} - K_5 \dot{\beta} & 0 \end{bmatrix}$$

$$K_1 = C_\beta S_\beta (C_\gamma^2 I_x + S_\gamma^2 I_y + I_z)$$

$$K_2 = C_\beta^2 C_\gamma S_\gamma (I_x - I_y)$$

$$K_3 = C_\gamma S_\gamma S_\gamma (I_x - I_y)$$

$$K_4 = \frac{1}{2} C_\beta (C_\gamma - S_\gamma) (C_\gamma + S_\gamma) (I_x - I_y)$$

$$K_5 = C_\gamma S_\gamma (I_x - I_y)$$

where  $I(\cdot)$  represent the inertia of the platform.

### III. Sliding Mode Controller Design

In this section we will illustrate the application of sliding mode controller on the inverse dynamics model in task space of (6-3) Gough-Stewart platform.

Sliding mode control approach consist of two steps; the first is the reachability phase and the second is sliding phase.

In reachability phase, states are being driven to a stable manifold, called sliding surface by means of appropriate control law. Thereafter, in sliding phase, states should stay on the surface while sliding to an equilibrium point.

The tracking control problem in task space is to find a control law such that given a desired trajectory  $P_{des}$ , the tracking error  $e_i$  tends to zero where:

$$e_i = P_m - P_{des} \quad (10)$$

The relative degree of the system  $r = 2$ , the sliding surface selected in our work is given by:

$$s = \lambda e + \dot{e} \quad (11)$$

where  $\lambda$  is  $6 \times 6$  diagonal positive definite matrix.

Keeping  $S$  equal to zero by an appropriate control law will lead to asymptotic stability of the system. Lyapunov direct method could be used to obtain the control law that stabilizes the system.

Consider the Lyapunov function candidate as:

$$V(S) = \frac{1}{2} S^T S \quad (12)$$

Time derivative of (12) will lead to:

$$\dot{V} = S^T \dot{S} \quad (13)$$

In which the term  $\dot{S}$  is given by:

$$\dot{s} = \lambda \dot{e} + \ddot{P}_m - \ddot{P}_{des} \quad (14)$$

From (5) the equation of inverse dynamic model in task space is written by:

$$\ddot{P} = M(P)^{-1} (J^T \Gamma - C(\dot{P}, P) \dot{P} - G(P)) \quad (15)$$

*Assumption 1:* The inertia matrix  $M$  is invertible.

*Assumption 2:* The mechanical system is designed so that the Jacobean matrix is nonsingular in the whole workspace. Taking (15) for  $\ddot{P}_m$  and substituting in (14) results in:

$$\dot{s} = M(P)^{-1} (J^T \Gamma - C(\dot{P}, P) \dot{P} - G(P)) - \ddot{P}_{des} + \lambda \dot{e} \quad (16)$$

Defining the control signal as:

$$\Gamma = \hat{\Gamma} - J^{-T} M K sgn(S) \quad (17)$$

where:

$$\Gamma = [\Gamma_1 \Gamma_2 \Gamma_3 \Gamma_4 \Gamma_5 \Gamma_6]^T$$

and  $\hat{\Gamma}$  is defined as:

$$\hat{\Gamma} = J^{-T} [M(P)(\ddot{P}_{des} - \lambda \dot{e}) + C(P, \dot{P}) \dot{P} + G(P)] \quad (18)$$

will cause:

$$\dot{S} = -K sgn(S) \quad (19)$$

where  $K \in R^{6 \times 1}$  is the gain and  $sgn(S)$  is switching function and respectively:

$$\dot{V} = -S^T K sgn(S) \leq 0 \quad (20)$$

Hence, according to the Lyapunov theory the control law (17) will result in a stable closed loop system. In practice, the control law (17) cannot be used because of containing the term  $sgn(S)$  which results in high frequency oscillations, called chattering, and it is replaced by a continuous approximation.

Chattering may be reduced by using a high saturation function. We define control law and tracking as:

$$\Gamma = \hat{\Gamma} - J^{-T} M K sat(S) \quad (21)$$

where  $sat(S)$  is a saturation function and can be defined as follow:

$$sat(s) = \begin{cases} \frac{s(t)}{\|s(t)\|} & \text{if } s > \delta \\ \frac{s(t)}{\|s(t) + \delta\|} & \text{if } s < \delta \end{cases} \quad (22)$$

which provide a very smooth control action.

#### IV. Simulation Results

In-order to examine the effectiveness of proposed controller Simulation has been performed. The platform can perform rotational and translation motion (surge, sway, heave, roll, pitch and yaw).

The simulation is carried out on a 6-3 Gough-Stewart platform model to verify the feasibility of the proposed control scheme.

The physical properties of the Stewart-Gough platform are considered as in Table I.

TABLE I  
PARAMETERS MODEL OF STEWART PLATFORM  
Parameters Values

Parameters Values	
<u>Mass (kg)</u>	
m	200 kg
<u>Platform inertial(kgm<sup>2</sup>)</u>	
I <sub>xx</sub>	30
I <sub>yy</sub>	30
I <sub>zz</sub>	60
g	9.81
<u>Nominal height of moving platformm</u>	
h	0.55

The position and orientation of upper platform P is determined by:

$$\begin{bmatrix} 0.3 \cos(\omega t) \\ 0.3 \sin(\omega t) \\ 0.2 + 0.55 \sin(\omega t) \\ 0 \\ 0 \\ 0 \end{bmatrix} [\text{m}]$$

The median position is selected as nominal operating point during simulation,  $P = [0 \ 0 \ 0.55 \ 0 \ 0 \ 0]^T$  [m].

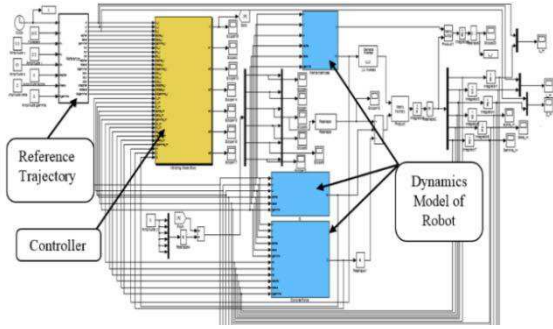


Fig. 2. Dynamic model with SMC of spatial 6-DOF parallel manipulator in Simulink

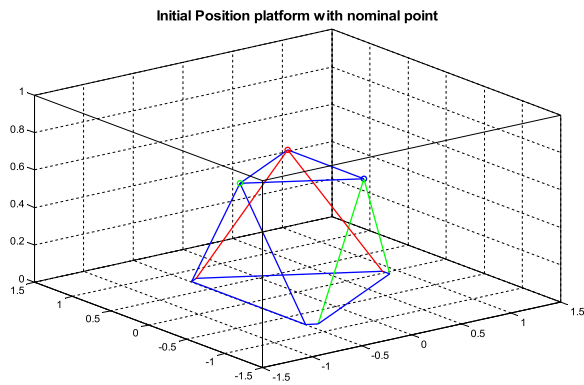


Fig. 3. Initial position of 6-3 flight simulator

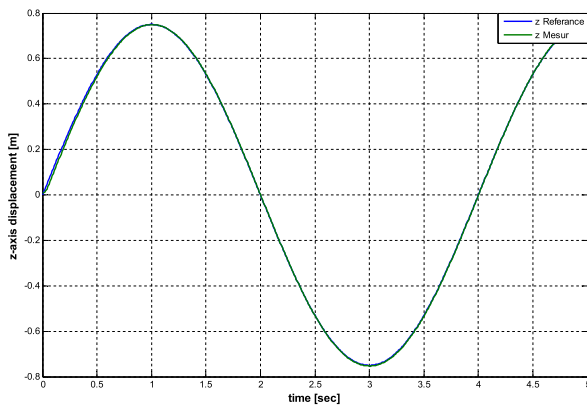


Fig. 4. The displacement of upper platform within Z-axis

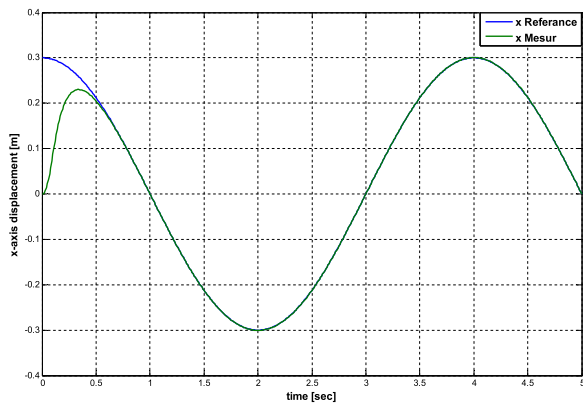


Fig. 5. The displacement of upper platform within X-axis

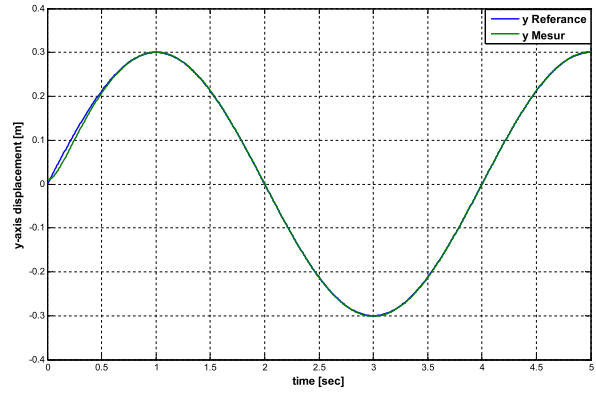


Fig. 6. The displacement of upper platform within Y-axis

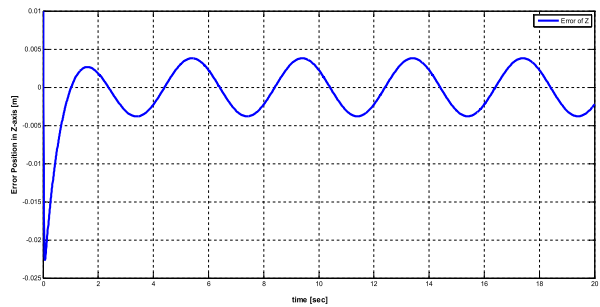


Fig. 7. Error position of upper platform within Z-axis

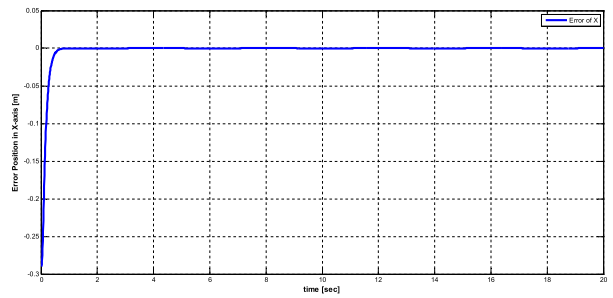


Fig. 8. Error position of upper platform within X-axis

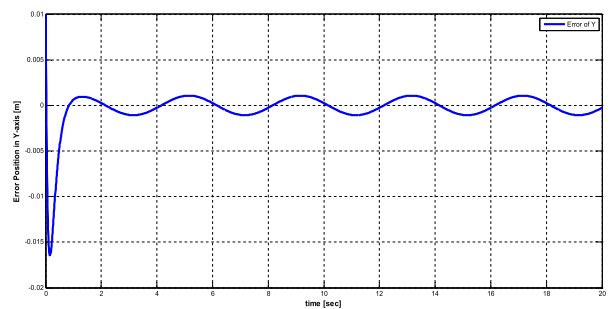


Fig. 9. Error position of upper platform within Y-axis

The simulation results illustrated in Fig. 4, Fig. 5, and Fig. 6 show a good displacement of upper platform with a good regulation in different axes.

In Fig. 4 the reference trajectory in z-axis is given as  $0.2 + 0.55 \sin(\omega t)$ , the platform is regulated in this position, with a good and same displacements of legs (active joints) illustrated in Fig. 7.

Fig. 7, Fig. 8, Fig. 9 show a good tracking of desired trajectories in x, y and z direction respectively with some variations of active joints presented in Fig. 11 and Fig. 12.

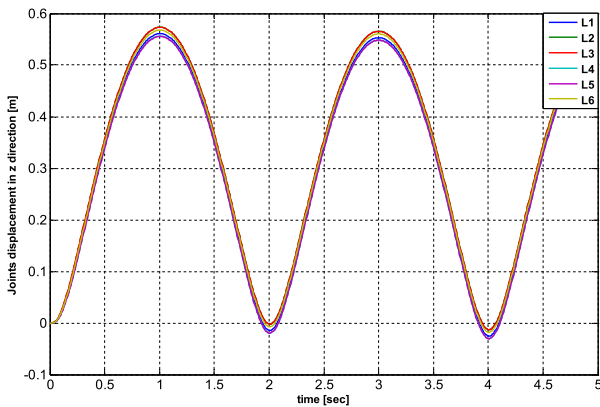


Fig. 10. Joint trajectory displacement with sliding mode control

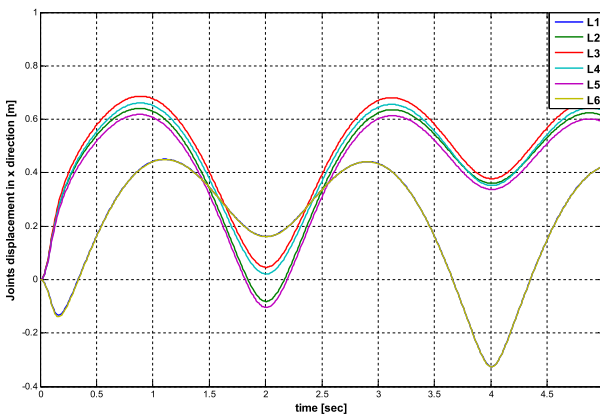


Fig. 11. Joint trajectory displacement with sliding mode control

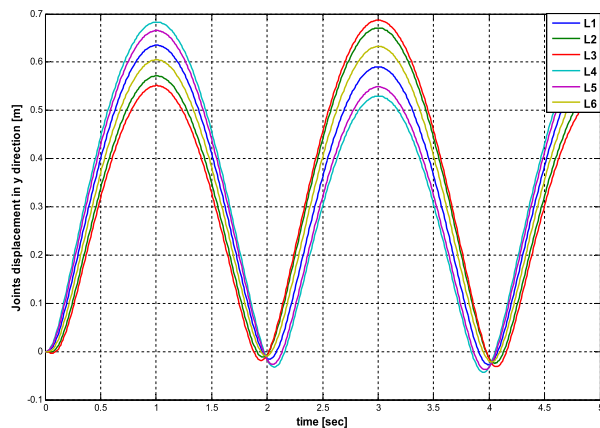


Fig. 12. Joints trajectory displacement with sliding mode control

## V. Conclusion

A sliding-mode controller design approach is used successfully for the regulation and tracking of a multi-input multi-output Gough-Stewart platform type. Stability analysis based on Lyapunov theory is performed

to guarantee global, asymptotic and exponential convergence. And some important properties of a dynamics of the Stewart platform have been derived to develop a sliding-mode controller which can drive upper platform angular and translation positions to the desired trajectories.

## References

- [1] V. E. Gough and S. G. Whitehall, *Universal type test machine*, in *Proc.9th Int. Tech. Congress FISITA*, pp. 117–137, 1962.
- [2] D. Stewart, A platform with six degree-of-freedom, in *Proc. Inst. Mech. Eng.*, vol. 180, pp. 371–386, 1965.
- [3] J.-Y. Kang, D. Kim, and K.-I. Lee, Robust Tracking Control of Stewart Platform, in *Proceedings of the 35th IEEE Decision and Control*, pp. 3014–3019, 1996.
- [4] M. R. Sirouspour and S. E. Salcudean, Nonlinear Control of aHydraulic Parallel Manipulator, in *Proceedings of IEEE International Conference on Robotics and Automation*, pp. 3760–3765, 2001.
- [5] I. Davliakos, and E. Papadopoulos, Model-based Control of a 6-dof electro hydraulic Stewart-Gough platform, *Mechanism and Machine Theory*, vol. 43, pp. 1385-1400,2008.
- [6] S.-H. Lee, J.-B. Song, W.-C. Choi, and D. Hong, Position Control of a Stewart Platform using inverse dynamics control with approximate dynamics, *Mechatronics*, vol. 13, pp. 605–619, 2006.
- [7] H. Hajimirzaalian, H. Moosavi, M. Massah, Dynamics Analysis and simulation of Parallel Robot Stewart Platform, in the *2nd International Conference on Computer and Automation Engineering (ICCAE)*, pp. 472 – 477, 2010.
- [8] Y. Ting, Y.-S. Chen, S.-M. Wang, Task-space Control algorithm for Stewart Platform, in *Proceedings of the 38th IEEE Conference on Decision and Control*, pp. 3857–3862, 1999.
- [9] S.-H. Lee, J.-B. Song, W.-C. Choi, and D. Hong, Controller design for a Stewart Platform using small workspace characteristics, in *Proceedings of the 2001 IEEE/RSJ International Conference on Intelligent Robots and Systems*, pp. 2184–2189, 2001.
- [10] Y. Ting, Y.-S. Chen, and H.-C. Jar, Modeling and Control for a Gough-Stewart platform CNC Machine, *Journal of Robotic Systems*, vol. 21, pp. 609–623, 2004.
- [11] C.-I. Huang, L.-C. Fu, Adaptive backstepping tracking control of the Stewart Platform, in *Proceedings of the 43rd IEEE Conference on Decision and Control*, pp. 5228–5233, 2004.
- [12] E. Yime, R. Saltaren, J. Diaz, Robust adaptive control of the Stewart-Gough robot in the task space, *American Control Conference (ACC)*, pp. 5248 – 5253, 2010.
- [13] F. Castañós, L. Fridman, Analysis and Design of Integral Sliding Manifolds for Systems with Unmatched Perturbations , *IEEE Transactions on Automatic Control*, Vol. 51, pp. 853-858, May 2006.
- [14] S.M. Nayeem Hasan and I. Husain, A Luenberger-Sliding Mode Observer for Online Parameter Estimation and Adaptation in High-Performance Induction Motor Drives, *IEEE Trans. on Ind. Appl.*, vol. 45, pp. 772-781, 2009.
- [15] J. Y. Hung, W. Gao, and J. C. Hung, Variable Structure Control: A Survey, *IEEE Transaction on Industrial Electronics*, Vol.40, pp. 2-19, Feb.1993.
- [16] F.J. Lin, S. Y. Chen, K. K. Shyu, Robust Dynamic Sliding-Mode Control Using Adaptive RENN for Magnetic Levitation System, *IEEE Trans. on Neural Networks*, vol. 20, pp. 938-951, 2009.
- [17] S. Islam and X. P. Liu, Robust Sliding Mode Control for Robot Manipulators, *IEEE Trans. on Ind. Electron.*, vol. 58, pp. 2444-2453, 2011.
- [18] S.C. Tan, Y.M. Lai, and C.K. Tse, General design issues of Sliding Mode Controllers in dc-dc converters, *IEEE Trans. on Ind. Electron*, vol. 55, pp. 1160-1174, 2008.
- [19] Messaoud, B., Amine, B.S., Mohammed, B., Boualem, N., Sliding mode controller design synchronized by PLL application to buck DC/DC converter, (2012) *International Review of Automatic Control (IREACO)*, 5 (5), pp. 567-574.
- [20] V. Sankaranarayanan, and A.D. Mahindrakar, Control of a Class

of Underactuated Mechanical Systems Using Sliding Modes, *IEEE Trans. on Robotics*, vol. 25, pp. 459-467, 2009.

- [21] Khiari, B., Sellami, A., Andoulsi, R., Mami, A., A novel strategy control of photovoltaic solar pumping system based on sliding mode control, (2012) *International Review of Automatic Control (IREACO)*, 5 (2), pp. 118-125.

### Authors' information

University of Sciences and Technology Mohamed Boudiaf, (USTO)  
Oran, Algeria.



**Mustapha Litim** was born in Oran Algeria in July 20. 1985. He received the diploma of Master degree on automation and control of intelligent industrial systems in 2009, from the automatic department, University of Sciences and Technology, Oran (USTO). Currently, he is a PHD Student at the (LDEE) laboratory of (USTO), Algeria. His research interests include

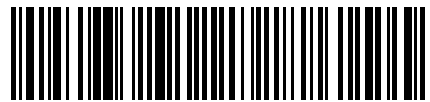
the robust control design on the nonlinear dynamic model of parallel manipulators.

**Abdelhafid Omari** received his PhD in Electrical Engineering from the University of Electro Communications in the city of Tokyo, Japan in 2001. He is currently working as an Associate Professor in the Faculty of Electrical Engineering at the University of Sciences and Technology in the city of Oran in Algeria. His research and teaching interests include: Automatic control, Intelligent Mechatronic Systems and Robotics control.





Praise Worthy Prize



1974-6067(201401)7:1;1-Y